Calculations for displacive ω-phase transformations in Ti–Al alloys with Nb additions at finite temperature

2008 J. Phys.: Condens. Matter 20 465206

(http://iopscience.iop.org/0953-8984/20/46/465206)

J. Phys.: Condens. Matter **20** (2008) 465206 (8pp) doi:10.1088/0953-8984/20/46/465206

Calculations for displacive ω-phase transformations in Ti–Al alloys with Nb additions at finite temperature

M Sanati[1,2], D West[1] and R C Albers[2]

[1] Physics Department, Texas Tech University, Lubbock, TX 79409, USA
[2] Theoretical Division, Los Alamos National Laboratory, Los Alamos, NM 87545, USA

E-mail: m.sanati@ttu.edu

Received 5 June 2008, in final form 26 September 2008
Published 21 October 2008
Online at stacks.iop.org/JPhysCM/20/465206

Abstract

We examine by means of first-principles calculations the bcc-like (bcc: body centered cubic) to ω-like phase transformations in Ti–Al alloys with Nb additions at finite temperature. To simulate the alloy we use different discrete atomic configurations in a six atom unit cell of the stoichiometry Ti_3Al_2Nb. Calculated ground state energies show an instability in the ternary Ti_3Al_2Nb alloy against the ω structure type atomic displacement. To better understand the role of entropy in the stability/instability of these systems, the first-principles calculations are extended to finite temperature by including various contributions to the free energy. In particular, the vibrational free energy is calculated within a quasiharmonic approximation. It is shown that the bcc structure is stabilized by the contribution of the low energy modes to the lattice entropy against ω type atomic displacements. We find that configurational entropy plays a major role in the ω to $B8_2$ transformation. Calculated lattice parameters and transition temperatures are found to be in excellent agreement with experiment.

(Some figures in this article are in colour only in the electronic version)

1. Introduction

Metastable states play an important role in the mechanisms for solid–solid displacive phase transformations (e.g., martensitic) [1, 2]. They involve the cooperative movement of atoms over small distances that are fractions of lattice translation vectors. In contrast, diffusion-controlled nucleation and growth transformations occur by the transport of atoms over much larger distances and longer times. Displacive transformations usually occur at lower temperatures than those involving diffusion, where there is less thermal energy for diffusion and reordering of the lattice, or due to rapid quenching where there is not enough time for diffusion processes to establish true equilibrium. They involve spontaneous distortions (strains) of the original unit cell (or a supercell of these) into a less symmetric structure with additional small movement of the atoms within the unit cell or supercell (these are usually called shuffles), as the system attempts to lower its free energy as best it can without the available thermal energy and kinetic driving forces to achieve true equilibrium. Displacive transformations have a significance that extends beyond their own particular study, since they can be viewed as a simple paradigm for more general complexity in materials.

While a number of zero-temperature first-principles studies have been done on these types of systems, less attention has been paid to the more difficult task of determining the effects of entropy on these transformations. Since almost all phase transformations occur at finite temperature, it is very important to consider the effects of thermal energy and whether they modify the results of zero-temperature band-structure calculations. Interest in developing such methods has, in particular, been appreciable for substitutional alloys [3].

In this regard the formation of the ω-phase [4] in elements (e.g., Ti) and alloys (e.g., Ti–Al–Nb and Ti–V), which was first reported by Frost *et al* [5] in 1954, forms almost a model system in which to study these types of effects because of its simplicity. These materials also have considerable technological importance, since Ti_3Al and TiAl alloys with Nb additions, in particular, have received a lot of attention as possible candidates in the search for light-weight materials

with the high temperature strength and low temperature ductility properties that are needed for aerospace applications. It should be noted that in β-Ti alloys [6] internal friction studies support a mechanism whereby the transformation is displacive rather than diffusional.

Among the Ti–Al alloys with Nb additions, alloys with a chemical composition near the stoichiometry of Ti_4Al_3Nb has been especially well characterized experimentally [7–13]. As the material is quenched and aged a series of ω-like transformations occur involving (i) B2 $\rightarrow \omega''$, (ii) $\omega'' \rightarrow B8_2$, and (iii) B2 $\rightarrow B8_2$. These will be described in greater detail below.

In this paper, we use first-principles calculations to investigate these transformations at finite temperature. Since we do no configurational averaging, we are forced to simulate the properties of the alloy through using specific discrete configurations. Since most of our calculations are done with the smallest reasonable unit cell (6 atoms per unit cell), we have examined configurations involving the alloy Ti_3Al_2Nb instead of Ti_4Al_3Nb. This alloy has the same Ti concentration as in the experimental work for Ti_4Al_3Nb [7, 8] (50%), but has a higher concentration of Nb at the expense of Al (16.7% instead of 12.5% Nb). Examining 6 atom cells with these alloy concentrations we are able to calculate the vibrational free energy within the quasiharmonic approximation and show that the vibrational entropy (as in transition metals) stabilizes the high temperature B2 phase. Also, the importance of the configurational entropy on the formation of the $B8_2$ phase in the $\omega'' \rightarrow B8_2$ transformation is discussed. We show that the theoretically calculated lattice parameters and transition temperatures are not affected by the enhanced Nb concentration that we used.

2. Crystal structure description

To understand the formation of the ω-type structures, it is useful to consider the atomic structure of the bcc lattice along the [111] direction (figure 1). In this direction the lattice appears as a series of three equally spaced planes of atoms that repeat periodically. The ω-type structures form out of the bcc-type lattices by a collapse of every second and third plane of the bcc lattice toward each other along the [111] direction while the distance between the first plane and its periodic replicas (e.g., the fourth plane) remains fixed. This is equivalent to a 2/3 longitudinal displacement phonon along the [111] direction. The ω-type structure [4] can involve either a partial or a full collapse of the second and third planes, called respectively an 'incomplete' (trigonal, structure type C6) or 'complete' (hexagonal, structure type C32) transformation[3]. When fully collapsed the ω crystal structure has only two periodically replicated planes.

When alloys containing different types of elements are formed in this crystal structure, the overall symmetry of the lattice, of course, depends on the placement of the atoms within the unit cell (or supercell) of the ω-type units. In alloys, some sites can also sometimes be occupied by a randomly disordered

[3] The NRL web site http://cst-www.nrl.navy.mil/lattice/ gives a useful description and pictures of these various lattices.

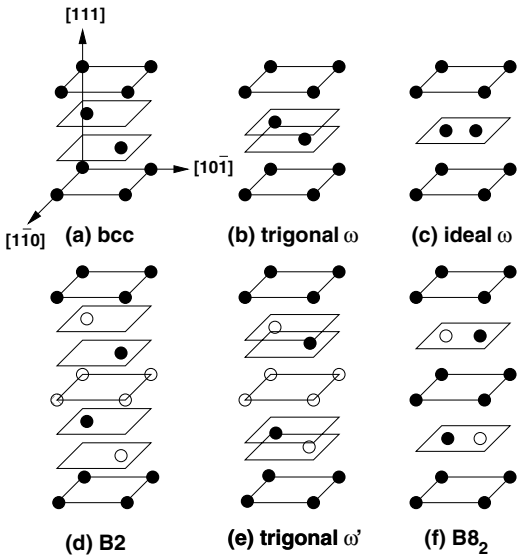

Figure 1. (a) Stacking of the (111) planes of bcc structure, (b) trigonal ω-phase (partial collapse of the planes), (c) ideal ω-phase (complete collapse of the planes), (d) B2 crystal structure which is doubled along the c-axis, (e) trigonal ω'-phase (partial collapse of the planes), (f) the $B8_2$ structure.

mixture of atoms from two or more different types of elements. This will not change the symmetry if completely disordered. Also, once the collapse of the second and third planes begin (figure 1), the original cubic symmetry is lost and the crystal structure can distort along the [111] direction to change the c/a ratio (the lattice constant a describing unit cell within the hexagonal-like planes within each plane and the lattice constant c the repeat distance of the unit cell along the original [111] direction).

The trigonal C6 incomplete ω-phase (shown in figure 1) is based on the $P\bar{3}m1$ space group (International Table No. 164). Its prototype is CdI_2 and has 3 atoms per unit cell: (1a) 0 0 0 and (2d) 1/3 2/3 1/2 + z and 2/3 1/3 1/2 − z. In the CdI_2 structure the Cd atoms occupy the (1a) Wyckoff position and the I atoms the (2d) positions. When $z = 0$, this crystal structure transforms into the hexagonal C32 complete ω structure (see below). When $z = 1/6$, it is equivalent to the bcc structure for $c/a = \sqrt{3/8}$ and a single atom type.

The hexagonal C32 complete ω-phase is based on the $P6/mmm$ space group (International Table No. 191). Its prototype is AlB_2 and has 3 atoms per unit cell: (1a) 0 0 0 and (2d) 1/3 2/3 1/2 and 2/3 1/3 1/2. The Al atoms occupy the (1a) Wyckoff position and the B atoms the (2d) positions.

A closely related phase is the $B8_2$ crystal structure (figure 1). This has a hexagonal ordered ω-like structure that is doubled along the c-axis, with two molecular units per unit cell. It has a $P6_3/mmc$ space group (International Table No. 194). Its prototype is Ni_2In and has 6 atoms per unit cell: (2a) 0 0 0 and 0 0 1/2, (2c) 1/3 2/3 1/4 and 2/3 1/3 3/4, and (2d) 1/3 2/3 3/4 and 2/3 1/3 1/4. The Ni atoms occupy the (2a) and (2d) Wyckoff positions and the In atoms the (2d) positions.

As noted by Bendersky *et al* [7], all of the relevant structures related to the ω-phases can be indexed on a $P\bar{3}m1$

space group (International Table No. 164), because it is a subgroup of all the others. We will follow this example in this paper, since all of the structures we examine can similarly be based upon this structure. In this general structure, following Bendersky *et al* [7], we have a doubled unit cell along the z-direction (figure 1) with 6 atoms per unit cell: (1a) 0 0 0, (1b) 0 0 1/2, (2d1) 1/3 2/3 z_1 and 2/3 1/3 1 $-$ z_1, and (2d2) 2/3 1/3 z_2 and 2/3 1/3 1 $-$ z_2. For our purposes we can use a single z and set (2d1) 1/3 2/3 1/6 + z and 2/3 1/3 5/6 $-$ z and (2d2) 2/3 1/3 1/3 $-$ z and 1/3 2/3 2/3 + z. This is arranged so that when $z = 0$ we have equally spaced planes (like bcc along the [111] direction for a single-element material), and when $z = 1/12$ the ω structure is fully collapsed with planes at 0, 1/4, 1/2, and 3/4. The different structures arise from different elements (or disordered mixtures of elements) occupying the different Wyckoff positions.

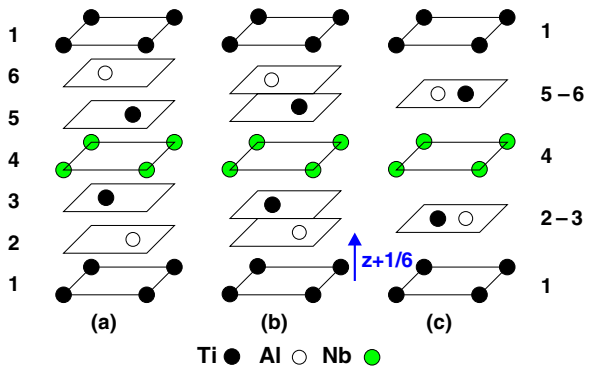

Figure 2. (Color online) (a) stacking of the (111) planes of underlying bcc Ti_3Al_2Nb structure (BOT) for $z = 0$, (b) trigonal ω''-phase (partial collapse of the planes) for $0 < z < 1/12$, (c) ω structure (full collapse of the planes) for $z = 1/12$.

3. Phase transformation description

The Ti–Al–Nb alloy system has a ductile disordered bcc or B2 (CsCl) phase over a wide range of composition at high temperatures. At lower temperatures ω-type and related $B8_2$ phases form. Depending on the morphology and microstructure of these phases they can either cause brittleness or help to strengthen the material [4]. In this class of materials both diffusion and displacement mechanisms can play a role in the formation of the various phases, as the material is either rapidly quenched or thermally equilibrated as it goes through different materials processes.

There have been a number of investigations of Ti_3Al alloys with Nb substitutions of up to 30 at.% for Ti. At high temperatures there is a bcc or B2 phase over this composition range. When quenching alloys at higher Nb concentrations (5–17 at.%), the bcc phase is found to order chemically to the B2 structure and then to age to a $B8_2$ structure. A particularly detailed study was done by Benersky *et al* [7] with further investigations by Sadi and Servant [8] for alloys with a chemical composition near the stoichiometry of Ti_4Al_3Nb. They found several phases appearing during cooling at various rates from the high temperature bcc phase field. These are the B2, $L1_0$, D019, and ω-type phase. The formation of a trigonal (incomplete) athermal ω-phase, called ω'' were reported by several experiments [7–13]; note that we agree with the arguments by de Fontaine and collaborators [14, 15] that there is no physical basis for differentiating between athermal and thermal ω-type phases, and we will treat both as the same. The ω'' structure is a partially-collapsed ω-phase with different site occupancies than what would occur for a direct 'ω-collapse' out of the disordered bcc alloy. Hence the sequence of phase transformations found by Bendersky *et al* [7] appears to be: chemically disordered bcc (A2) $\rightarrow$ ordered B2 $\rightarrow$ ω'' $\rightarrow$ isothermal ω-phase ($B8_2$).

A direct transformation from the B2($Pm\bar{3}m$) to the $B8_2$($P6_3/mmc$) structure would be strongly first-order due to symmetry, since $P6_3/mmc$ is not a subgroup of $Pm\bar{3}m$. Instead, the observed path, B2 $\rightarrow$ ω'' $\rightarrow$ $B8_2$, traverses a state of minimum symmetry through the ω'' ($P\bar{3}m1$) that is a subgroup of both $Pm\bar{3}m$ and $P6_3/mmc$. The formation of ω'' as an intermediate metastable phase thus provides a continuous structural path for the alloy to accomplish the B2 to $B8_2$ transition.

In the alloys the structure is only fully determined when the site occupancies are specified. The sites can be occupied by a single element or by disordered mixtures of several elements. In the B2 or bcc-like phase, the occupancy reported by Banerjee *et al* [16] showed that Ti tends to occupy one site while Al and Nb tend to occupy the other site. The measured site occupancies of the ω''-phase indicate that the phase transformation first involve a change in chemical order with a transfer of Nb atoms out of collapsing planes (figure 2) into stationary ones [7]. It is suggested that the absence of the Nb atoms from the collapsing planes is because of the strong interaction between Ti and Al atoms (due to considerably large negative heat of mixing between them). Therefore, transition-metal–Al interactions are the origin of the both the A2 $\rightarrow$ B2 ordering and the ω-phase formation in the B2 phase of TiAl–X (X = Nb, V) system [7, 19, 20]. In this paper we do not examine the chemical ordering aspects of this phase transformation, but instead focus on the displacive transformation of the lowest energy configuration.

4. Methodology

The present calculations have been carried out using first-principles density-functional packages, VASP [21–24], within the generalized gradient approximation to the exchange–correlation potential [25]. The VASP calculations use a plane-wave basis set and ultrasoft Vanderbilt type pseudopotentials [26]. In the VASP approach, the solution of the generalized self-consistent Kohn–Sham equations are calculated using an efficient matrix-diagonalization routine based on sequential band-by-band residual minimization method and Pulay-like charge density mixing [27]. We used a plane-wave basis cutoff at 321 eV for all structures. Electronic degrees of freedom were optimized with a conjugate gradient algorithm, and both cell constants and ionic positions are fully relaxed. The crystal is represented by 6 or 12 atom periodic cells. The 7 $\times$ 7 $\times$ 5 and 7 $\times$ 7 $\times$ 3 Monkhorst–Pack [28]

mesh are used to sample the Brillouin zone of 6 and 12 atom cells, respectively. The dynamical matrix calculations were done using force-constant method in a 108 atoms cell with k-point sampling of $2 \times 2 \times 2$.

The eigenvalues of the dynamical matrix are the normal-mode frequencies ω_s of the system. The knowledge of all normal modes of the supercell also allows the construction of the phonon density $g(\omega)$. This function is obtained by evaluating the dynamical matrix at 10 000 k points in the Brillouin zone of the supercell. Once $g(\omega)$ is known, the Helmholtz vibrational free energy F_{vib} is straightforward to calculate [29–31].

5. $T = 0$ results

In order to understand the properties of an alloy within a specific 6 atom unit cell from first-principles calculations, it is necessary to specify the placement of each type of atom (element) within this unit cell. The various unit cells and chemical orderings that we have considered are shown in figure 2. We have constrained the c/a ratio to be $\sqrt{6}/2$ (the ideal value). For this c/a the material can continuously transform into the bcc or B2 structures when the chemical order is set appropriately. The lattice constant a can be determined by minimizing the total energy.

After studying all the possible arrangements of atoms in the 6 atom unit cell, we find that that the atomic configuration in figure 2(a) has the lowest energy. For convenience, from now on, the structure shown in figure 2(a) will be referred to as the body center orthogonal ternary (BOT) structure (note that this is the bcc-like equally spaced plane version of the crystal structure with $z = 0$). In terms of the general description of the crystal structure given in section 2, Ti atoms occupy the Wyckoff sites (1a) and (2d2), the Al atoms the site (2d1), and the Nb atoms the site (1b). The overall stoichiometry is Ti_3Al_2Nb, which has the same Ti concentration as in the experimental work for Ti_4Al_3Nb [7, 8] (50%), but has a higher concentration of Nb at the expense of Al (16.7% instead of 12.5% Nb). Our BOT structure is in agreement with experiment [16] in that Ti atoms tends to occupy one site while Al and Nb tend to occupy the other sites of the B2 structure. Note that the B2 structure has a site occupancy with the (1a) and (2d2) sites being filled with one type of atom and the (1b) and (2d1) sites with atoms of the other type.

After the overall unit cell dimensions and atomic configurations were determined, we then varied the positions of the planes along $(111)_{\text{bcc}}$ and calculated the total energy versus plane displacement, z (figure 2) (where z is a dimensionless variable varying between 0 and 1/12 in terms of c/a unit) (figure 3). The lattice with $z = 0$ corresponds to a bcc structure. The complete ω-phase is formed when $z = 1/12$; for the other values of z, the structures are the 'incomplete' ω-phase (ω''). Finally the structure parameters were optimized around the minima of the energy (figure 3). Calculated atomic parameters for BOT and ω'' and their comparison with experiment are shown in table 1. The calculated parameters are in an excellent agreement with experiment.

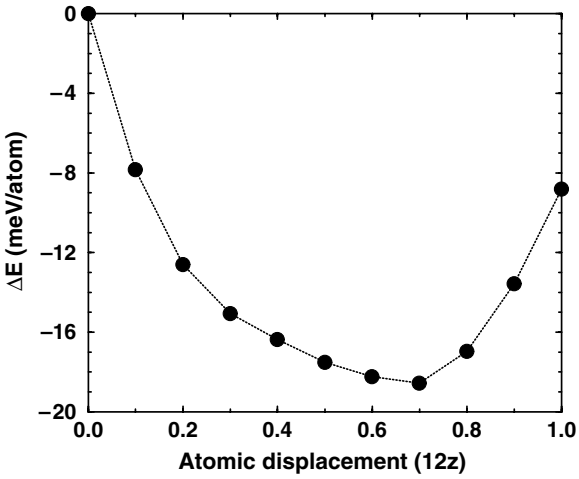

Figure 3. Calculated total energy as a function of atomic displacement for the Ti_3Al_2Nb system.

Table 1. Calculated and experimental values for atomic parameters of Ti_3Al_2Nb BOT and ω'' structures. The experimental values for BOT and ω'' structures are taken from [8] and [10], respectively.

	BOT (exp.)	BOT (calc.)	ω'' (exp.)	ω'' (calc.)
a (Å)	3.224	3.229	4.555	4.609
c (Å)			5.542	5.479
$z + 1/6$	0	0	0.2245	0.2335

The instability of the BOT structure with respect to the ω-type displacement is a consequence of the strong bonding between the Ti and Al atoms. Pair-potential modeling for the Ti_3Al_2Nb system [32] and first-principles studies of transition metal aluminides [33, 34] indicate the existence of a strong covalent bonding component, which makes the bonding between Ti–Al atoms significantly stronger than between Ti–Nb or Al–Al atoms. This statement is in agreement with the results of the x-ray photoelectron spectroscopy (XPS) studies of Ti–Al and Ti–Al–V alloys [35] that indicate charge transfer from the Al sites towards the transition metal sites. The Ti–Al bond is stronger at shorter distances, relative to their positions in BOT structure. Therefore, one expects to see the instability of the BOT structure toward the ω-phase. In this way, the Ti–Al bond can reduce its energy.

Since the BOT structure is unstable at zero temperature to an ω instability, this raises the question of why it is experimentally found to be the stable structure at high temperature? Entropy-driven structural phase transformations have been found in a number of alloys [36, 37] besides elements like titanium [38] and zirconium [39], which suggests that the BOT structure of Ti_3Al_2Nb system can also be stabilized by excess (vibrational) entropy at high temperature. In section 6 we extend our studies to finite temperatures by calculating the relevant thermodynamical potentials from first-principles.

6. Finite temperature results

The thermodynamical quantity determining the phase stability for fixed P and T (pressure and temperature of the system,

respectively) is the Gibbs free energy $G(P, T)$. However, in the case where all calculations are carried out near the equilibrium volume ($P \approx 0$), it becomes a good approximation to use the Helmholtz free energy instead of the Gibbs free energy. Since quasiharmonic phonon calculations (see below) are performed at fixed volume, this approximation simplifies the calculations. To determine the effects of entropy at high temperatures, one must consider the different possible contributions to the entropy such as electronic, vibrational, and configurational.

The electronic contribution to the free energy depends on the electronic density of states as a function of volume, $n(E, V)$. The occupation of these states, given by the Fermi distribution $f(E, T) = [e^{(E-E_f)/(K_B T)} + 1]^{-1}$, determines their entropy [40]

$$S_{el}(T, V) = -k_B \int [f \ln f + (1 - f)\ln(1 - f)] n(E, V)\, dE \quad (1)$$

and hence the electronic contribution to the free energy $F_E(T, V) = -T S_{el}(T, V)$. Although the electronic entropy terms are not large, we include them in our calculations for completeness.

The vibrational modes of the crystal are usually a much more important contribution to the free energy of the system than the electronic contribution. Significantly far below the melting point (when the anharmonicities get very severe), the vibrational free energy F_{vib} can be calculated within the quasiharmonic approximation. This is similar to calculating F_{vib} in the harmonic approximation, but retaining only the implicit volume dependence through the frequencies as [41]

$$F_{vib}(T, V) = 3k_B T \int_\Omega \ln\left\{2\sinh\left(\frac{\hbar\omega}{2k_B T}\right)\right\} g(\omega, V)\, d\omega. \quad (2)$$

We have calculated the phonon density of states at a few volumes and interpolated to get the volume dependence. The quasiharmonic approximation accounts only partially for the effects of the anharmonicity through the volume dependence of the phonon spectra. However, this is often a very good approximation at temperatures not too close to the melting point [42, 43]. At very high temperatures or very close to melting, to go beyond this approximation would either require anharmonic expansions [44], which may not converge, or self-consistent phonon theories [45, 46], which would increase the complexity of the calculations by one or several orders of magnitude. For this reason they are rarely attempted [43, 47–49]. They are certainly beyond the scope of this paper.

6.1. *B2 → (athermal) ω″ transformation*

Figure 4 shows the difference between the Helmholtz free energies of the BOT and ω'' (or incomplete ω) structures. Above 1336 K the bcc-like BOT structure is more stable than ω''-phase. The transmission electron microscopy analysis of similar alloy concentration indicates that the decomposition of the B2 phase occurs only below the 1373 K [7, 16] which is in excellent agreement with the calculated transition temperature.

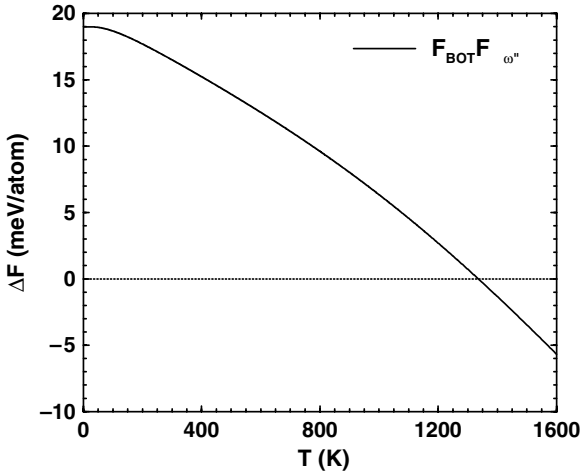

Figure 4. The total free energy difference of BOT and ω''-phase as a function of temperature. Below 1336 K the ω''-phase is more stable than BOT. Note that the z used for the ω''-phase is fixed to be the same as the zero-temperature minimum energy structure ($Z + 1/6 = 0.2327$).

In figure 5, the phonon density of states for BOT and ω'' at the predicted transition temperature is shown. The calculated phonon density of states consists of two bands separated by a gap for both structures. The Ti and Nb related modes are at low and Al at high energies (frequencies). In BOT structures phonons in both bands are shifted to the lower frequencies with respect to the ω''-phase. The high frequency modes are due to the strong bonding between the Ti and Al atoms and change of the nearest neighbors atoms with respect to the BOT structure. Therefore, we support the model by Friedel [17] that the excess entropy for the bcc phase is due to an overall lower phonon spectrum, expected to scale with the number of neighbors. We found small imaginary vibrational frequency for BOT structure along [111] direction at 2/3 2/3 2/3 (figure 6). This is the expected soft phonon for bcc to ω-phase transformation. First-principles study of the bcc phase of transition metal elements (TME) shows the similar instability in phonon dispersion along [111] direction [18]. In general presence of the imaginary frequencies indicates that the structure is dynamically unstable. However, there is a major difference between the instability in BOT system and the TME. We found a very small imaginary frequency (less than 1% of the maximum frequency along [111] direction) in a small region of the Brillouin zone. While, calculated phonon dispersion for TME of imaginary phonons are more than 50% of the calculated maximum frequencies and in a much larger region of the Brillouin zone. Therefore, a free energy calculation in TME within harmonic approximation is less reliable [18] than BOT. The fact that phonon dispersion only barely touches the axis indicates that the region of unstable phonons is almost vanishingly small, and hence it is still a good approximation to ignore this bad point and calculate the free energy as we do for a thermodynamic solid. The good agreement between the calculated transformation temperatures and experimental values justifies this procedure.

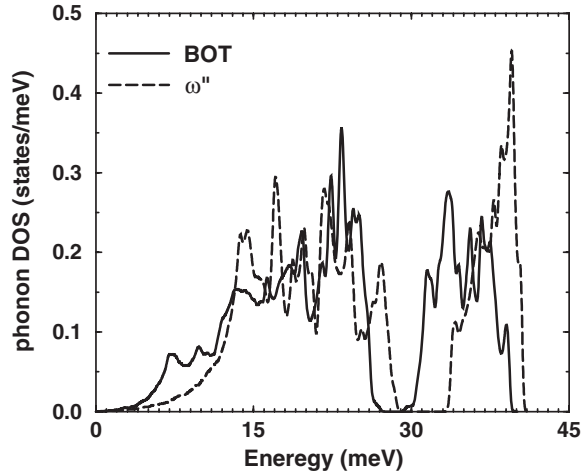

Figure 5. The phonon DOS for B2 (solid line) and ω'' (dashed line) phases at $T = 1336$ K.

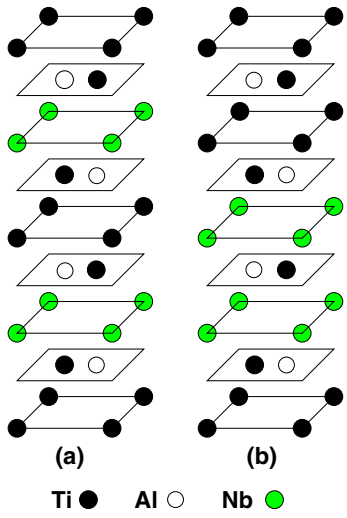

Figure 7. (Color online) The two different atomic configurations of the $B8_2$ structure with the lowest ground state energies.

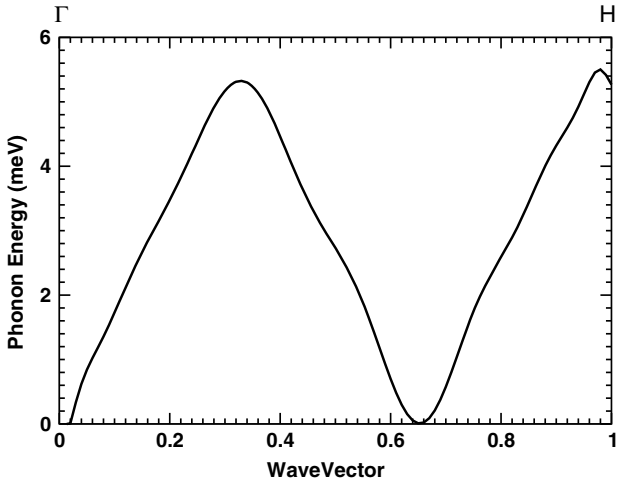

Figure 6. The phonon dispersion along [111] for BOT phase at $T = 1336$ K.

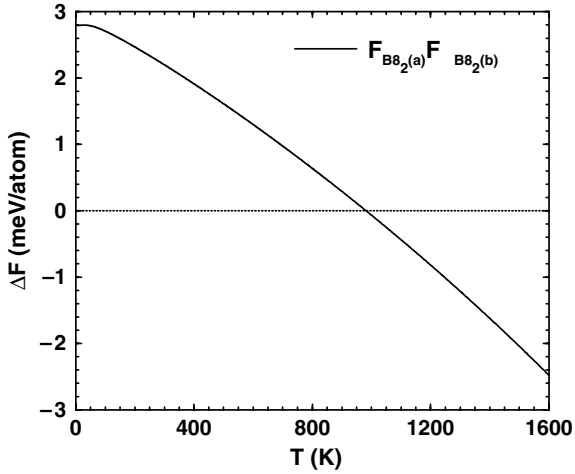

Figure 8. The total free energy difference between $B8_2$(a) and (b) structures. The calculated transition temperature is at 982 K. The $B8_2$(a) configuration is stable above the transition temperature while $B8_2$(b) is more stable below 982 K.

6.2. ω'' → (isothermal) $B8_2$ transformation

Annealing of the ω''-phase at 973 K results in another metastable structure known as $B8_2$ (an isothermal, complete ω phase) [7]. In the $B8_2$ structure, the double layers (planes 2–3 and 5–6 in figure 2(c)) are composed of Ti and Al with all of the Nb found on the single layers [7]. In figure 2(c), one of the possible configuration of the $B8_2$ is shown. The exchange of the Nb atoms in the fourth plane with Ti atoms in the first plane does not create a new configuration due to periodic boundary condition and translational symmetry of the crystal. Therefore, one needs to consider a bigger unit cell, and we have therefore considered possible 12 atom configurations, which involve the next largest size of unit cell that preserves stoichiometry.

The two lowest energy 12 atom configurations are shown in figure 7. These distinct configurations are called $B8_2$(a) and (b). The ground state energy calculations show that $B8_2$(a) has 4 meV/atom higher energy than $B8_2$(b). However, comparison of the Helmholtz free energy of both structures reveals that the $B8_2$(a) structure is more stable above 982 K (figure 8). The phonon density of the states is shown in figure 9. One can see a major change in the low energy region of the phonon density of states while the high energy region is not affected. This can be easily explained in terms of the chemical bonding between the atoms. The $B8_2$(a) structure has more Ti–Nb bonds with respect to the (b) structure. It is known that Ti–Nb bond is the weakest bond in Ti–Al–Nb system [32, 50]. Therefore, by rearranging the atomic configurations from $B8_2$(a) to (b) the weak Ti–Nb bonds are replaced by more stable Ti–Ti and Nb–Nb bonds that results in a shift to higher frequencies.

At 982 K, both structures have the same energy and one needs to include the contribution of the configurational entropy from both configurations to the total free energy of the system. Assuming that these are the only important configurations, the configurational contribution to the free

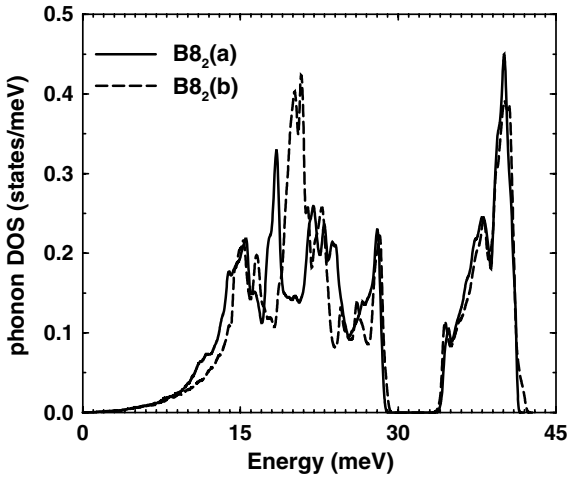

Figure 9. The phonon DOS for $B8_2$ (a) (solid line) and (b) (dashed line) phases at $T = 982$ K.

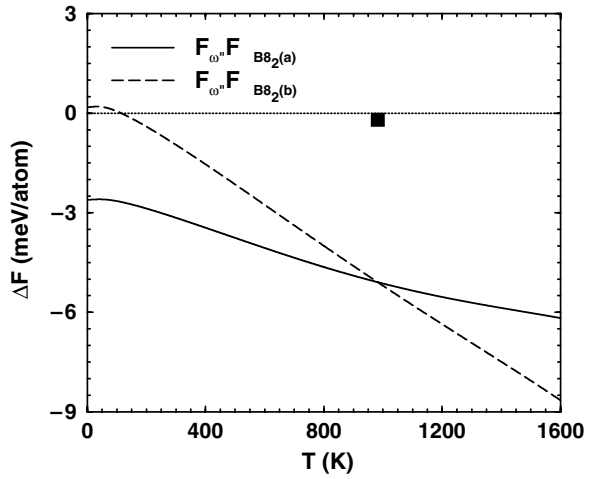

Figure 10. The difference between the total free energies of ω''-phase with $B8_2$(a) (solid line) and $B8_2$(b) (dashed line). The square indicates the free energy difference when configurational entropy is included.

energy is equal to $-TS_{\text{config}} = -K_{\text{B}}T\ln 2/12$ per atom. Note that this contribution is only included at $T = 982$ K where both structures are degenerate. In figure 10 the free energy difference between the ω'' and $B8_2$s without contribution of configurational entropy is depicted. We see from this figure that ω'' is more stable than $B8_2$(a) structure at all temperatures while $B8_2$(b) is slightly stable below 115 K by only 0.2 meV/atom. However, when the configurational entropy is included, the ω''-phase is more stable than $B8_2$ structure by only 0.2 meV/atom at 982 K which is very small number and within the error of our calculations. It is important to mention that we cannot find similar degeneracy for ω''-phase within the 12 atom cell configuration. Consequently, we predict 982 K as the transformation temperature for $\omega'' \rightarrow B8_2$ which is in excellent agreement with the measured value of 973 K [51].

6.3. $B2 \rightarrow$ (isothermal) $B8_2$ transformation

The direct equilibrium transformation of $B2 \rightarrow B8_2$ without the formation of the intermediate trigonal phase can only occur by a reconstructive transformation. In fact, during the cooling the BOT phase transform into the isothermal ω-phase at 1046 K [51]. Calculated transformation temperatures from BOT to $B8_2$(a) and (b) (figure 11) are 1061 and 1049 K, respectively which are in excellent agreement with experiment.

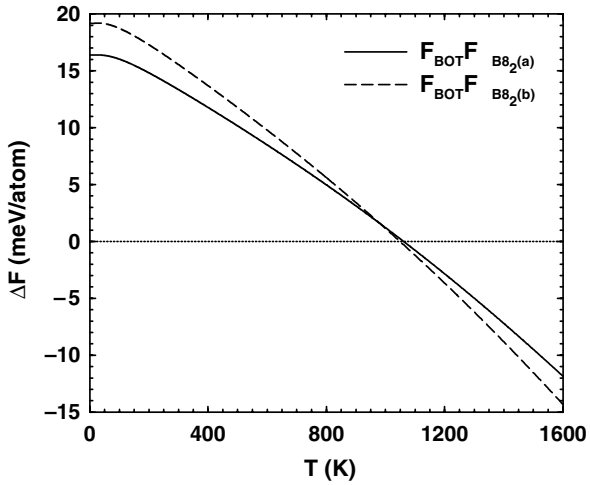

Figure 11. The difference between the total free energies of BOT and $B8_2$(a) (solid line) and $B8_2$(b) (dashed line) as a function of the temperature.

7. Conclusions

We have performed first-principles calculations to study the stability of the underlying bcc, ω'', and $B8_2$ structures of the Ti_3Al_2Nb system. The various contributions to the free energy of different metastable phases are calculated. The vibrational free energy is obtained from first-principles in the quasiharmonic approximation. The electronic entropy contribution to the free energy for all of the phases is calculated. The phonon density of states for each structure at transition temperatures is calculated. Predicted transition temperatures and lattice parameters for different phases are in excellent agreement with experiment.

It is confirmed that BOT $\rightarrow$ $B8_2$ transformation can be obtained from two different transition sequences. In the first sequence, in the first step the B2 matrix transforms to an intermediate trigonal phase. This is a subgroup transition during the cooling, with displacive mode which produces a metastable intermediate phase ω''. It is shown that the high temperature underlying bcc structure is stabilized by low frequency phonons. The second step involves a supergroup transition during the prolonged annealing with replacive mode and chemical ordering, which produces the equilibrium $B8_2$ phase from the ω''-phase. The site occupancies which are different in ω'' become identical in $B8_2$, and this implies an increase in configurational entropy. It is verified that the configurational entropy is indeed the major factor in this step of the transition. We showed that the underlying bcc structure

is stabilized by excess vibrational entropy against ω'' and $B8_2$ phases. It was also shown that for the $\omega'' \rightarrow B8_2$ transformation it is necessary to include the configurational entropy. In the second sequence, the direct BOT $\rightarrow$ $B8_2$ transformation occurs by a reconstructive transformation without the formation of the intermediate ω''-phase.

Acknowledgments

This work was carried out under the auspices of the Advanced Research Program of the State of Texas and the National Nuclear Security Administration of the US Department of Energy at Los Alamos National Laboratory under Contract No. DE-AC52-06NA25396. The generous amounts of computer time provided by Texas Tech's High Performance Computer Center was much appreciated.

References

[1] Wayman C M and Bhadeshia H K D H 1996 Phase transformations, nondiffusive *Physical Metallurgy* 4th edn, ed R W Cahn and P Haasen (Amsterdam: North-Holland) p 1507
[2] Olson G B and Owen W S 1992 *Martensite* (Materials Park, OH: ASM International)
[3] van de Walle A and Cedar G 2002 *Rev. Mod. Phys.* **74** 11
[4] Sikka S K, Vohra Y K and Chidambaram R 1982 *Prog. Mater. Sci.* **27** 245
[5] Frost P D, Parris W M, Hirsch L L, Doig J R and Schwartz C M 1954 *Trans. Am. Soc. Met.* **46** 231
[6] Sommer A W, Motokura S, Ono K and Buck O 1973 *Acta Metall.* **21** 489
[7] Bendersky L A, Boettinger W J, Burton B P and Biancaniello F S 1990 *Acta Metall. Mater.* **38** 931
[8] Sadi F A and Servant C 2000 *Phil. Mag.* A **80** 639
[9] Yu T H and Koo C H 1997 *Mater. Sci. Eng.* A **239/240** 694
[10] Shoemaker C B, Shoemaker D P and Bendersky L A 1990 *Acta Crystallogr.* C **46** 374
[11] Banerjee D, Gogia A K, Nandi T K and Joshi V A 1988 *Acta Metall.* **36** 871
[12] Strychor R, Williams J C and Soffa W A 1988 *Metall. Trans.* A **19** 225
[13] Chang C P and Loretto M H 1991 *Phil. Mag.* A **63** 389
[14] de Fontaine D, Paton N E and Williams J C 1971 *Acta Metall.* **19** 1153
[15] Williams J C, de Fontaine D and Paton N E 1973 *Metall. Trans.* **4** 2701
[16] Bendersky L A, Burton B P, Boettinger W J and Biancaniello F S 1990 *Scr. Metall.* **24** 1541
[17] Friedel J 1974 *J. Phys. Lett.* **35** L59
[18] Souvatzis P, Eriksson O, Katsnelson M I and Rudin S P 2008 *Phys. Rev. Lett.* **100** 095901
[19] Shao G and Tsakiropoulos P 2002 *Mater. Sci. Eng.* A **329–331** 914
[20] Shao G, Miodownik A P and Tsakiropoulos P 1995 *Phil. Mag.* A **71** 1389
[21] VASP 2003 http://cms.mpi.univie.ac.at/vasp
[22] Kresse G and Hafner J 1993 *Phys. Rev.* B **47** 558
[23] Kresse G and Furthmüller J 1996 *Phys. Rev.* B **54** 11169
[24] Kresse G and Joubert D 1999 *Phys. Rev.* B **59** 1758
[25] Perdew J P 1991 *Electronic Structure of Solids '91* ed P Ziesche and H Eschring (Berlin: Akademie) p 11
[26] Vanderbilt D 1990 *Phys. Rev.* B **41** 7892
[27] Kresse G and Furthmüller J 1996 *Comput. Mater. Sci.* **6** 15
[28] Monkhorst H J and Pack J D 1976 *Phys. Rev.* B **13** 5188
[29] Sanati M, West D and Albers R C 2007 *J. Phys.: Condens. Matter* **19** 386221
[30] Estreicher S K, Sanati M, West D and Ruymgaart F 2004 *Phys. Rev.* B **70** 125209
[31] Rudin S P, Jones M D and Albers R C 2004 *Phys. Rev.* B **69** 094117
[32] Sanati M and Albers R C 2006 unpublished
[33] Sanati M, West D and Albers R C 2007 *Phys. Rev.* B **76** 174101
[34] Nguyen-Manh D and Pettifor D G 1999 *Intermetallics* **7** 1095
[35] Diplas S, Watts J F, Tsakiropoulos P, Shao G, Beamson G and Matthew J A D 2001 *Surf. Interface Anal.* **31** 734
[36] Entel P, Meyer R, Kadau K, Herper H C and Hoffmann E 1998 *Eur. Phys. J.* B **5** 379
[37] Rubini S and Ballone P 1993 *Phys. Rev.* B **48** 99
[38] Petry W, Heiming A, Trampenau J, Alba M, Herzig C, Schober H R and Vogl G 1991 *Phys. Rev.* B **43** 10933
[39] Heiming A, Petry W, Trampenau J, Alba M, Herzig C, Schober H R and Vogl G 1991 *Phys. Rev.* B **43** 10948
[40] Watson R E and Weinert M 2001 *Solid State Physics* vol 56, ed H Ehrenreich and F Spaepen (San Diego, CA: Academic) p 85
[41] Baroni S, de Gironcoli S, Dal Corso A and Giannozzi P 2001 *Rev. Mod. Phys.* **73** 515
[42] Kern G, Kresse G and Hafner J 1999 *Phys. Rev.* B **59** 8551
[43] Moleko L K and Glyde H R 1983 *Phys. Rev.* B **27** 6019
[44] Glyde H R and Klein M L 1971 *Crit. Rev. Solid State Sci.* B **2** 181
[45] Wallace D C 1972 *Thermodynamics of Crystals* (New York: Wiley)
[46] Choquard P F 1967 *The Anharmonic Crystal* (New York: Benjamin)
[47] Albers R C and Gubernatis J E 1981 *Phys. Rev.* B **23** 2782
[48] Shukla K, Paskin A, Welch D O and Dienes G J 1981 *Phys. Rev.* B **24** 724
[49] Jayanthi C S, Tosatti E and Fasolino A 1985 *Phys. Rev.* B **31** 470
[50] Moffat D L and Kattner U R 1988 *Metall. Trans.* A **19** 2389
[51] Sadi F A and Servant C 2000 *Z. Metallkd.* **91** 504